A Porous-Medium Approach for Modeling Heart Mechanics.* I. Theory

SHAUL SOREK AND SAMUEL SIDEMAN†
The Julius Silver Institute of Biomedical Engineering,
Technion — Israel Institute of Technology, Haifa, 32 000, Israel

Received 7 November 1985; revised 20 March 1986

ABSTRACT

A method is developed for evaluating the distribution of the blood pressure, stresses and strains of the muscle fibers, and motion of the cardiac wall due to the cyclic contractions of the heart. The cardiac system is subdivided into two media: the chambers and the wall; the latter is enclosed by two impermeable surfaces (with one interface separating the two media and the other confining the wall). The momentum balance equation for the blood in the (two) cardiac ventricles is averaged, yielding a modification of Forchheimer's law, namely inclusion of the time derivative of the flux. The contracting muscle provides the driving force for the blood flow, and the endocardial velocity is thus taken as identical to that of the blood in the cavity next to the wall. Translation of the endocardium is governed by the blood pressure gradients in the ventricles. The blood pressure and stress-strain pattern in the myocardium are analyzed by applying concepts of the theory of mixtures to the blood and to the saturated solid matrix. With the blood pressure simulated by a modified Darcy law with relative fluid-solid velocity, fiber stresses and strains can be assessed with the aid of appropriate constitutive and compatibility laws.

INTRODUCTION

Insight into cardiac fluid dynamics, and into heart mechanics in general, necessitates detailed quantitative measurement of the cardiac system parameters in time and space. This, however, is an extremely difficult undertaking in view of the complex anatomic arrangement of the cardiac fibers, and of the interaction of blood rheology and tissue mechanics in the course of the cyclic contraction. The geometry of the heart also plays an important role in this context [5, 9]: its shape and size are unique for every human being,

*Supported by a grant from the Michael Kennedy-Leigh Fund and sponsored by the MEP Group, Women's Division, ATS, New York.

†R. J. Matas/Winnipeg Professor of Biomedical Engineering.

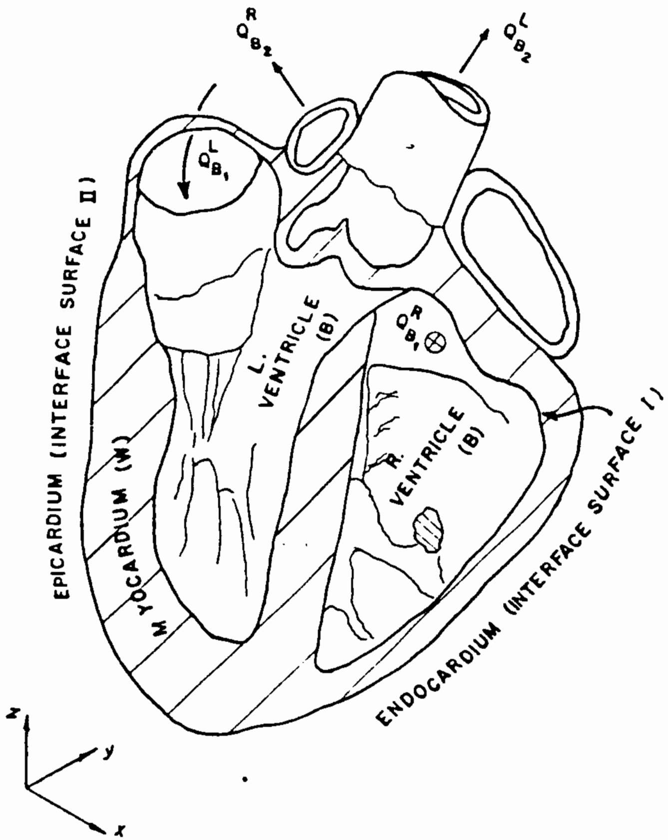

FIG. 1. Heart system.

undergoing changes while maturing and affected by disease [2]. Heethaar et al. [4] developed a regional model for computing cardiac wall mechanics, whereby Darcy's law was extended to incorporate specific flow patterns through individual blood vessels and a statistical approach is used to assess the flow regime in the rest of the myocardium.

In the present study the heart (i.e. the two ventricles) is taken to consist of two domains: one fluid controlled (the cavities) and the other a two-phase composite which comprises the myocardium encasing the cavities, (Figure 1). The two domains are obviously interlinked; they affect each other via their matched boundary conditions along the endocardium, and are characterized

by different regional properties which determine their mechanical behavior within the continuum.

Realizing the interactions between blood flow, stresses, and deformations [6], cardiac-mechanics relationships are derived here by evaluating the fluid-solid interactions in representative elementary "control" volumes in both cavities and in the wall. The blood momentum balance in the cavities is spatially averaged [8, 11] to yield, together with its mass balance, the distribution of the blood pressure and velocity profiles. The calculated pressure gradients are then used to describe the associated endocardial displacements. The myocardium is replaced by a single-phase fictitious entity described by combined mass and momentum balance equations [1, 10]. Thus, a modified Darcy law using relative fluid-solid motion is obtained. Blood pressure gradients and solid-inertia terms define the driving forces for the distribution of the stresses in the "saturated" solid. A possible extension of this approach will be to designate individual blood vessels as boundary segments in the discretized cardiac wall, thereby providing a better tool for describing the flow-stress relationships under various operating conditions and local disturbances.

A. FLOW IN THE VENTRICULAR CAVITIES

We first describe the flow regime in the cardiac cavities (Section B in Figure 1). The flow is assumed to be governed by Reynolds numbers of the order of a few hundred. The blood is assumed incompressible, body forces do not exist, and shear stresses within the cavity are negligible.

MASS BALANCE

The mass continuity equation for a fluid without flux sources is written as

$$\frac{\partial}{\partial t} n_B + \nabla \cdot (n_B \mathbf{v}_B) = 0, \tag{1}$$

where n_B = effective porosity, $\mathbf{v}_B$ = velocity vector.

MOMENTUM BALANCE

Fluid momentum conservation for each direction $\mathbf{l}$ dictates

$$\frac{\partial}{\partial t}(\rho^F v_{Bl}) + \nabla \cdot (\rho^F \mathbf{v}_B v_{Bl}) = -\mathbf{l} \cdot \nabla p_B \tag{2}$$

where v_{Bl} = velocity in B directed towards $\mathbf{l}$, ρ^F = fluid specific mass, p_B = blood pressure in B.

Equation (2) is usually extremely difficult to solve numerically. For the assumed low range of Reynolds numbers and with the aid of representative local space averaging procedures, it reads [8, 11]

$$aq_B^2\mathbf{A} + b|q_B|\mathbf{B} + c\left|\frac{\partial q_B}{\partial t}\right|\mathbf{C} = -\nabla\psi_B, \tag{3}$$

where

$$q_B = n_b v_b \quad \text{(flux)}, \tag{4.1}$$

$$\psi_B = \frac{p_B}{\rho^F g} \quad \text{(pressure head)}, \tag{4.2}$$

and

$$a = \frac{1-n_B}{n_B^3}\cdot\frac{1}{gV_{sB}}, \tag{5.1}$$

$$b = \frac{(1-n_B)^2}{n_B^3}\cdot\frac{\mu/\rho^F}{gV_{sB}^2}, \tag{5.2}$$

$$c = \frac{1}{n_B g}. \tag{5.3}$$

Here, V_{sB} is the volume of the solid portion in B; g is the acceleration of gravity; μ/ρ^F is the kinematic viscosity, μ being the dynamic viscosity; and $\mathbf{A}$, $\mathbf{B}$, and $\mathbf{C}$ are vectors incorporating the direction cosines and the shape factors of the pores. Note that the term $c(\partial q_B/\partial t)$ becomes operative the instant there is an abrupt change in flux.

Let q_B^* be the new "flux level" following transition from the preceding level because of $c(\partial q_B/\partial t)$. By virtue of Equation (3) we may write

$$(aq_B^* + b^*)\mathbf{q}_B^* \cong -\nabla\psi_B + d^* \tag{6.1}$$

where b^*, d^* are the new values attained after approximating the term $\partial q_B/\partial t$. Using, for example, a backward difference scheme, we obtain

$$b^* = b + \frac{c}{\Delta t}, \tag{6.2}$$

$$\mathbf{d}^* = \frac{c}{\Delta t}\mathbf{q}_B^k. \tag{6.3}$$

Here, Δt = time difference between two ascending time levels (time step); $(\ )^k$ = value at preceding time level. Thus, in view of (6) a modified Forchheimer formula results:

$$\mathbf{q}_B^* = n_B\mathbf{v}_B = -Z\nabla\psi_B^* \tag{7.1}$$

$$Z = Z(\nabla\psi_B) = \frac{1}{\dfrac{b^*}{2} + \sqrt{\left(\dfrac{b^*}{2}\right)^2 + a|\mathbf{d}^* - \nabla\psi_B|}} \tag{7.2}$$

THREE-DIMENSIONAL EQUATIONS

With the notion that the cavity's porosity is mainly a function of the pressure head, $n_B = n_B(\psi_B)$, we define a fluid specific capacity C_B as

$$C_B = \frac{dn_B}{d\psi_B}. \tag{8}$$

By virtue of Equations (1) and (7) we obtain the blood-flow equation

$$C_B\frac{\partial\psi_B^*}{\partial t} = \nabla\cdot(Z\nabla\psi_B^*). \tag{9}$$

Equation (9) is subject to the initial condition

$$\psi_B^*(\mathbf{x},0) = \psi_{B_0}(\mathbf{x}), \tag{10}$$

where $\mathbf{x}$ = spatial position vector; and to the boundary condition

$$-Z\nabla\psi_B^*\cdot\mathbf{n} + \alpha_\Gamma(\psi_B^* - \psi_{B_\Gamma}) = Q_{B_\Gamma}, \tag{11}$$

where Γ = enclosing surface at each time level, $\mathbf{n}$ = unit vector normal to Γ and pointing outwards. $\psi_{B_0}, \psi_{B_\Gamma}, Q_{B_\Gamma}$ are prescribed functions and control the type of boundary conditions: a Dirichlet condition when

$$\psi_B^* = \psi_{B_\Gamma}, \qquad \alpha_\Gamma \to \infty, \tag{12}$$

a Neumann condition when

$$-Z\nabla\psi_B^*\cdot\mathbf{n} = Q_{B_\Gamma}, \qquad \alpha_\Gamma = 0, \tag{13}$$

and a mixed condition when

$$0 < \alpha_\Gamma < \infty. \tag{14}$$

The equation describing the movement of the endocardium will now be derived. This translation will be shown to be due to the blood pressure gradients in the ventricles.

B. INTERFACE I

Let us denote the system of interfaces as a whole by $H(\mathbf{x}, t)$, the endocardium by H_1, and the epicardium by H_2.

No mass is transferred through H_1, yet certain jump conditions prevail. With a viscous fluid, on either side, in the cavity, and one in the saturated muscle matrix, the no-slip condition dictates

$$[\mathbf{q} \cdot \boldsymbol{\tau}] = 0, \tag{15}$$

where $[\ ]$ denotes the jump in a quantity and τ is a unit tangent vector. The fluid motion normal to the interface is dictated by the interfacial velocity $\dot{\mathbf{x}}$; thus

$$(\mathbf{v} - \dot{\mathbf{x}}) \cdot \mathbf{n} = 0, \tag{16}$$

where n is a unit normal vector pointing outward. The Pressure is continuous through the interface:

$$[p] = 0. \tag{17}$$

The general equation for the interfaces is

$$z = H_{(\mathbf{x},t)}. \tag{18}$$

The values for n and τ are thus

$$\mathbf{n} = \left[\left(\frac{\partial H}{\partial x}\right)^2 + \left(\frac{\partial H}{\partial y}\right)^2 + \left(1 - \frac{\partial H}{\partial z}\right)^2\right]^{-1/2} \left(\frac{\partial H}{\partial x}, \frac{\partial H}{\partial y}, 1 - \frac{\partial H}{\partial z}\right) \tag{19}$$

$$\boldsymbol{\tau} = \left[\left(\frac{\partial H}{\partial x}\right)^2 + \left(\frac{\partial H}{\partial y}\right)^2 + \left(1 - \frac{\partial H}{\partial z}\right)^2\right]^{-1/2} \left(1, 1, \frac{\frac{\partial H}{\partial x} + \frac{\partial H}{\partial y}}{1 - \frac{\partial H}{\partial z}}\right). \tag{20}$$

By virtue of (18) we obtain

$$\frac{Dz}{Dt} = \frac{DH}{Dt} = \frac{\partial H}{\partial t} + \dot{\mathbf{x}} \cdot \nabla H. \tag{21}$$

From the point of view of the ventricles (the "balloon" part), and bearing in mind (7.1), Equation (21) is rewritten to read

$$\frac{\partial H_1}{\partial t} = \left(\frac{Z}{n_B} \nabla \psi_B^*\right) \cdot \nabla (H_1 - z). \tag{22}$$

Equation (22) is to be solved for H_1 subject to

$$H_1(\mathbf{x}, 0) = H_{1_0}(\mathbf{x}). \tag{23}$$

Define a time differentiation operator as

$$\frac{\mathscr{L}}{\mathscr{L}t} = \frac{\partial}{\partial t} - \left(\frac{Z}{n_B} \nabla \psi_B^*\right) \cdot \nabla. \tag{24}$$

In view of (24), Equation (22) is rewritten to read

$$\frac{\mathscr{L} H_1}{\mathscr{L}t} = -\frac{Z}{n_B} \nabla \psi_B^* \cdot \nabla z. \tag{25}$$

Note that unlike Equation (22), H_1 in Equation (25) follows characteristic paths defined by

$$\frac{\mathscr{L}\mathbf{x}}{\mathscr{L}t} = -\frac{Z}{n_B} \nabla \psi_B^*. \tag{26}$$

Thus its translation can be described by forward tracking of particles conveying H_1 values.

C. MECHANICS OF THE MYOCARDIUM

The cardiac wall is regarded as a fully saturated porous medium undergoing finite movements. The fluid phase here lumps together all the extracellular fluid, including the blood circulatory network in the muscle matrix. It is assumed that a finite movement can be regarded as the accumulation of small displacements. The evolution of the wall mechanics will be assessed for each such displacement. The specific mass of the solid portion is assumed incompressible. Fluid shear stress is disregarded.

Let σ be the mixture solid-fluid stress, σ^s effective solid skeleton stress, and p the fluid pressure at the pores. Then

$$\sigma = \sigma^s - p. \tag{27}$$

Given that the ratio of relaxation time to activation time is very small, we have

$$\frac{\partial \sigma^s}{\partial t} - \frac{\partial p}{\partial t} = \frac{\partial \sigma}{\partial t} \to 0, \tag{28.1}$$

or

$$d\sigma^s = dp. \tag{28.2}$$

The fluid and solid volumes V_w^s, V_w^F are expressed respectively by

$$V_w^F = n_w V_w^b, \tag{29.1}$$

$$V_w^s = (1-n_w)V_w^b = \text{const}, \tag{29.2}$$

where V_w^b, the bulk volume, is the sum of both:

$$V_w^b = V_w^s + V_w^F. \tag{29.3}$$

Define

$$\alpha = \frac{1}{V_w^b}\frac{\partial V_w^b}{\partial \sigma^s}. \tag{30.1}$$

Thus by virtue of (28.2) and (29.2), Equation (30.1) may be written as

$$\alpha = \frac{1}{1-n_w}\frac{\partial n_w}{\partial \sigma^s} = \frac{1}{1-n_w}\frac{\partial n_w}{\partial p}. \tag{30.2}$$

Hence, the time derivative of the porosity $n_w = n_w(\sigma^s, p)$ is

$$\frac{\partial n_w}{\partial t} = \frac{\partial n_w}{\partial p}\frac{\partial p}{\partial t} + \frac{\partial n_w}{\partial \sigma^s}\frac{\partial \sigma^s}{\partial t} = C_w\frac{\partial \psi_w}{\partial t}, \tag{40.1}$$

where

$$c_w = 2\frac{\partial n_w}{\partial \psi_w}; \qquad \psi_w = \frac{p_w}{\rho^F g}. \tag{40.2}$$

MASS BALANCE

Conservation of mass for fluid and solid respectively dictates

$$\frac{\partial n_w}{\partial t} + \nabla\cdot(n_w \mathbf{v}^F) = 0, \tag{41}$$

$$\frac{\partial(1-n_w)}{\partial t} + \nabla\cdot[(1-n_w)\mathbf{v}^s] = 0. \tag{42}$$

Adding and rearranging, we obtain

$$\frac{\partial n_w}{\partial t} + \nabla\cdot(\mathbf{q}_w + n_w\mathbf{v}^s) = 0, \tag{43}$$

$$\nabla\cdot\mathbf{q}_w + \nabla\cdot\mathbf{v}^s = 0, \tag{44}$$

where

$$\mathbf{q}_w = n_w(\mathbf{v}^F - \mathbf{v}^s). \tag{45}$$

EQUATIONS OF MOTION

Following Biot [1], we replace the two-phase system by a fictitious single-phase entity. The force balance (momentum balance) equations for the solid and the fluid phases, respectively, are

$$\sigma_{ij,i} + \rho^s b_i^s = \frac{\partial^2}{\partial t^2}\left(\rho^{ss}u_i^s + \rho^{sF}u_i^F\right) - \mathbf{R}\frac{\partial}{\partial t}\left(u_i^F - u_i^s\right), \tag{46}$$

$$\sigma_{,i} + \rho^F b_i^F = \frac{\partial^2}{\partial t^2}\left(\rho^{sF}u_i^s + \rho^{FF}u_i^F\right) + \mathbf{R}\frac{\partial}{\partial t}\left(u_i^F - u_i^s\right), \tag{47}$$

where σ is the stress due to fluid pressure,

$$\sigma = -n_w p_w; \tag{48.1}$$

σ_{ij} is the stress due to the solid's stress (T_{ij}),

$$\sigma_{ij} = (1-n_w)T_{ij}; \tag{48.2}$$

$\rho^{ss}, \rho^{sF}, \rho^{FF}$ are the specific mass coefficients,

$$\rho^{ss} = (1-n_w)\rho^s - \rho^{sF}, \tag{48.3}$$

$$\rho^{FF} = (1-n_w)\rho^F - \rho^{sF}, \tag{48.4}$$

$$\rho^{sF} < (1-n_w)\sqrt{\rho^s\rho^F}; \tag{48.5}$$

b_i is the body force per unit mass; u_i is the average displacement; and $\mathbf{R}$ is the resistance tensor.

Let us now introduce the following assumptions:

(1) The mass coupling factor is too small to be effective, i.e.,

$$\rho^{sF} \to 0. \tag{49.1}$$

(2) No body forces affect the solid or fluid mass, i.e.,

$$\mathbf{b}^s = 0 \tag{49.2}$$

and

$$\mathbf{b}^F = 0. \tag{49.3}$$

(3) The fluid inertia term is negligibly small, i.e.,

$$\frac{\partial^2}{\partial t^2}\left(\rho^{FF}u_i^F\right) \to 0. \tag{49.4}$$

In view of Equations (45), (47)–(49), we obtain

$$\mathbf{q}_w = -\left(g\rho^F n_w \mathbf{R}^{-1}\right)\nabla\left(n_w \frac{p}{g\rho^F}\right) = -\mathbf{k}\nabla(n\psi_w). \tag{50}$$

From Equations (40), (43), (50) the resulting flow equation is

$$C_w \frac{\partial \psi_w}{\partial t} = \nabla\cdot\left[\mathbf{k}\nabla(n_w\psi_w) - n_w\mathbf{v}^s\right]. \tag{60}$$

Suppose now that we know the solid's velocity, $\mathbf{v}^s$, from a previous evaluation, say

$$\mathbf{v}^s = \tilde{\mathbf{v}}^s. \tag{61}$$

Moreover, in view of (40.2) we may write

$$\nabla n_w = \frac{\partial n_w}{\partial \psi_w}\nabla\psi_w = \tfrac{1}{2}C_w\nabla\psi_w; \tag{62}$$

hence by virture of (61) and (62), Equation (60) yields

$$C_w \frac{\partial \psi_w}{\partial t} = \nabla\cdot\left[\mathbf{k}\nabla(n_w\psi_w)\right] - \tfrac{1}{2}C_w\tilde{\mathbf{v}}^s\cdot\partial\psi_w. \tag{63}$$

Also, by virtue of Equations (44) and (50), the solid continuity equation is

$$\nabla\cdot\mathbf{v}^s = \nabla\cdot\left[\mathbf{k}\nabla(n_w\psi_w)\right]. \tag{64}$$

In view of (62), Equation (50) can be rewritten as

$$\mathbf{q}_w = -\mathbf{k}'\nabla\psi, \tag{65}$$

where

$$\mathbf{k}' = \left(n_w + \tfrac{1}{2}C_w\psi_w\right)\mathbf{k} = g\rho^F n_w\left(n_w + \tfrac{1}{2}C_w\psi_w\right)\mathbf{R}^{-1}. \tag{66}$$

Thus, by substituting Equation (65) in (63) and (64), we obtain the motion equations for the fluid and solid respectively:

$$C_w \frac{\partial \psi_w}{\partial t} = \nabla\cdot(\mathbf{k}'\nabla\psi_w) - \tfrac{1}{2}C_w\tilde{\mathbf{v}}^s\cdot\nabla\psi_w, \tag{67}$$

$$\nabla\cdot\mathbf{v}^s = \nabla\cdot(\mathbf{k}'\nabla\psi_w). \tag{68}$$

Let us now deal with the stress distribution in the solid portion of the cardiac wall. Differentiating Equation (45) with respect to time and relating

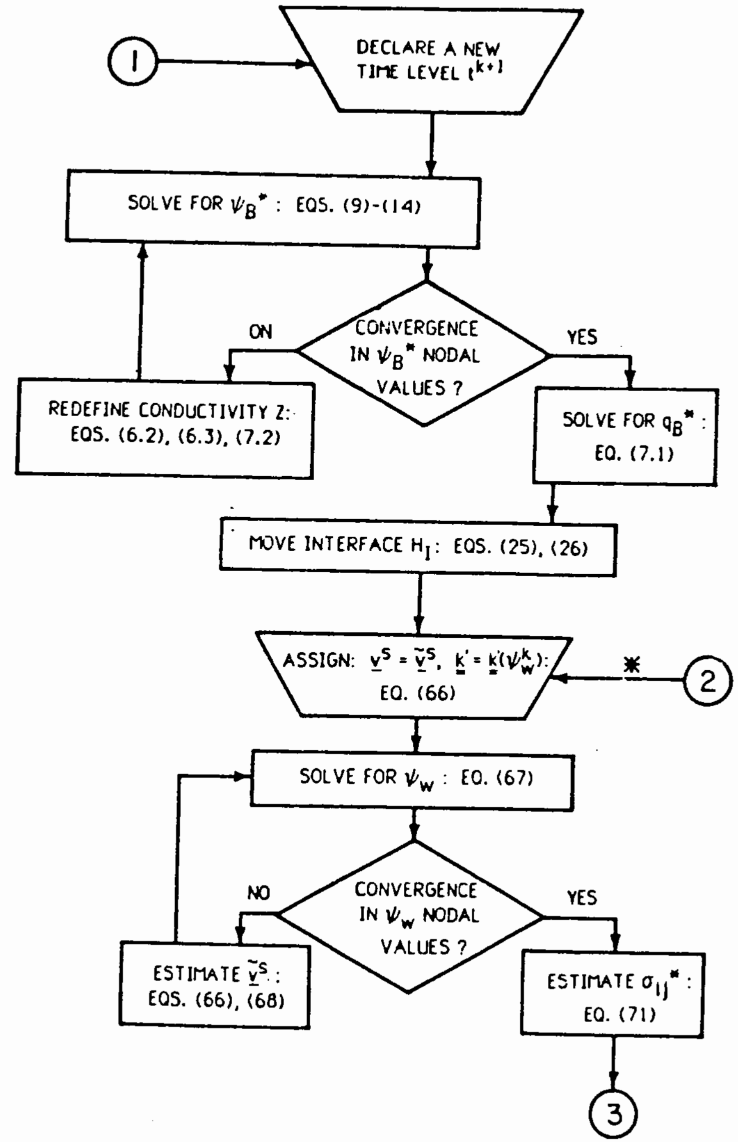

FIG. 2. Proposed iteration scheme to evaluate the cardiac system.

it to Equations (40.1) and (49.4), we obtain

$$\frac{\partial^2 \mathbf{u}^s}{\partial t^2} = \frac{C_w}{n_w^2}\frac{\partial \psi_w}{\partial t}\mathbf{q}_w - \frac{1}{n_w}\frac{\partial \mathbf{q}_w}{\partial t}. \tag{69}$$

By adding Equations (46) and (47), and bearing in mind (40.1), (48.1), (48.3), (49.2), and (69), the force balance equation for the solid matrix yields

$$\begin{aligned}\sigma_{ij,i} = {} & \rho^F g\left(n_w + \tfrac{1}{2}C_w\psi_w\right)\psi_{w,i} \\ & + \rho^s \frac{1-n_w}{n_w^2}\left[C_w \frac{\partial \psi_w}{\partial t} q_{w_i} - n_w \frac{\partial q_{wi}}{\partial t}\right] - \rho^s u_i^s \frac{\partial}{\partial t}\left(C_w \frac{\partial \psi_w}{\partial t}\right). \end{aligned} \tag{70}$$

Note that on omitting the last term in the right-hand side of Equation (70), we obtain an equation that can now be used to evaluate $\sigma^*_{ij,i}$, the approximate value of $\sigma_{ij,i}$:

$$\sigma^*_{ij,i} = \rho^F g\left(n_w + \tfrac{1}{2}C_w\psi_w\right)\psi_{w,i} + \rho^s \frac{1-n_w}{n_w^2}\left[C_w \frac{\partial \psi_w}{\partial t} q_{w_i} - n_w \frac{\partial q_{w_i}}{\partial t}\right]. \tag{71}$$

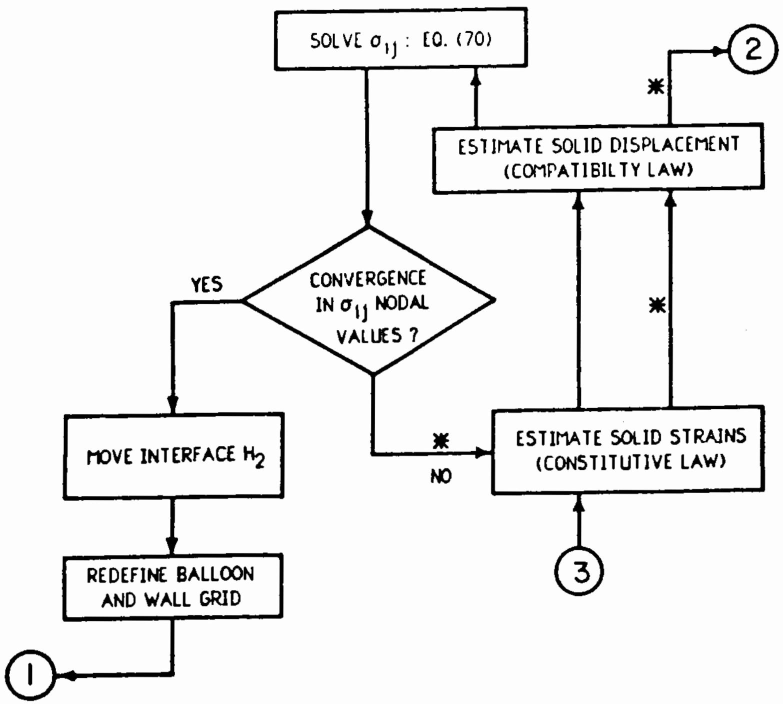

FIG. 2. (*Continued*)

The mechanical behavior of the cardiac system has been evaluated for each period of the cycle. The motion of blood in the ventricular cavities is subject to the inflow-outflow flux conditions, and the displacement of the endocardium is incompatible with blood pressure gradients at the cavities. The stresses and blood pressure in the myocardium are thus interlinked and activated by the motion of the endocardium and the pressure exerted on it by the blood in the cavities. The proposed iteration scheme for evaluating heart mechanics within each time step is presented in Figure 2.

D. CONCLUSION

A porous-medium approach to the cardiac system is suggested here as a new and convenient tool for evaluating the stresses, strains, and blood flow distribution in the cavities and the ventricular wall. For the cavities, the blood momentum balance is averaged and reformulated to yield Forchheimer's law with inertial terms. A governing equation for displacements of the endocardium is established by using pressure gradients along it. The cardiac wall is considered as a two-phase (solid-fluid) system, and the governing equations are derived on the basis of Biot's mixture theory.

The novelty of this work lies in treating the cardiac system as a dynamic solid-fluid interaction subject to boundary conditions such as inflow-outflow flux at the ventricles and the coronary tree.

REFERENCES

1 M. A. Biot, Theory of finite deformations of porous solids, *Indiana Univ. Math. J.* 21:797–620 (1972).
2 A. C. Burton, The importance of the shape and size of the heart, *Amer. Heart J.* 54:801–810 (1957).
3 A. C. Guyton, *Textbook of Medical Physiology*, 6th ed., 1981.
4 R. M. Heethaar, J. Heethar, and J. M. Huyghe, Cardiac imaging and modelling, in *Proceedings of the Workshop on Three-Dimensional Simulation and Imaging of the Cardiac System*, Technion, Israel, Mar. 1984.
5 R. M. Heethaar, Y. C. Pao, and E. L. Ritman, Computer aspects of three dimensional finite element analysis of stresses and strains in the intact heart, *Comput. Biomed. Res.* 10:271–285 (1977).
6 J. I. E. Hoffman, The effect of intramyocardial forces on the distribution of intramyocardial blood flow, *J. Biomed. Engrg.* 1:33–40 (1979).
7 J. M. Huyghe, A continuum approach to blood-tissue interaction in the myocardium, Scientific report, Twente Univ. of Technol., The Netherlands, 1984.